# Optically produced arrays of planar nanostructures inside fused silica

Bhardwaj, V. R.; Simova, E.; Rajeev, P. P.; Hnatovsky, C.; Taylor, R. S.; Rayner, D. M.; Corkum, P. B.



**Publisher's version / Version de l'éditeur:**
https://doi.org/10.1103/PhysRevLett.96.057404
*Physical Review Letters, 96, 5, pp. 057404-1-057404-4, 2006-02-07*

# Optically Produced Arrays of Planar Nanostructures inside Fused Silica

V. R. Bhardwaj,[1,*] E. Simova,[1] P. P. Rajeev,[1] C. Hnatovsky,[2] R. S. Taylor,[3] D. M. Rayner,[1,†] and P. B. Corkum[1,‡]

[1]*Steacie Institute for Molecular Sciences, National Research Council, 100 Sussex Dr, Ottawa, K1A 0R6, Canada*
[2]*Department of Physics, University of Ottawa, 150 Louis Pasteur, Ottawa, K1N 6N5, Canada*
[3]*Institute for Microstructural Sciences, National Research Council, 1200 Montreal Rd., Ottawa, K1A 0R6, Canada*
(Received 28 April 2005; revised manuscript received 11 August 2005; published 7 February 2006)

Linearly polarized femtosecond light pulses, focused inside fused silica to an intensity that leads to multiphoton ionization, produce arrayed planes of modified material having their normal parallel to the laser polarization. The planes are $\leq 10$ nm thick and are spaced at $\sim\lambda/2$ in the medium for free space wavelengths of both 800 and 400 nm. By slowly scanning the sample under a fixed laser focus, order is maintained over macroscopic distances for all angles between the polarization and scan direction. With the laser polarization parallel to the scan direction we produce long-range Bragg-like gratings. We discuss how local field enhancement influences dielectric ionization, describe how this leads to nanoplane growth, why the planes are arrayed, and how long-range order is maintained.

DOI: 10.1103/PhysRevLett.96.057404 PACS numbers: 78.67.−n, 33.80.Rv, 73.20.Mf, 81.16.Rf

We observe arrayed $\leq$10 nm wide nanoplanes inside fused silica formed in the focal region of a $\sim$50 femtosecond Ti:sapphire laser beam. These structures are formed despite the fact that the focal spot of a laser beam is limited in free space optics to about a wavelength. We propose that local field enhancements play a critical role in their formation. In nanoplasmonics, the local field enhancement near a metal-dielectric interface [1,2] overcomes the diffraction limit of light. Electric fields can be concentrated to nanometer scale leading to light confinement well below laser wavelengths.

High intensity femtosecond laser pulses focussed inside the bulk material lead to plasma formation through multiphoton ionization. The plasma density grows during the laser pulse. During much of the critical growth period the plasma is underdense [3]. Any inhomogeniety in the plasma formation will lead to local field enhancements that must influence subsequent growth. If the inhomegenities are highly localized, they lead to the formation of nanoplasmas in the dielectric. The nanoplasmas drive structural changes that are imprinted in the material.

Nanoplasmonics has not been considered in conventional models of dielectric breakdown with short [4] or ultrashort [5] pulses—nanostructures are hard to observe inside dielectrics and plasmas are hard to diagnose. We observe the nanostructures by cutting or grinding the dielectric to the modified zone and polishing and etching the surface before imaging it with an atomic force microscope (AFM) [6] or a scanning electron microscope (SEM). These techniques reveal the modification through the differential etch rate between the modified and unmodified regions. They have a resolution of 20 and 5 nm, respectively.

Evidence of nanostructures has been previously found for a stationary focus by polishing to reveal a cross section of the laser-modified regions and imaging them by electron backscattering [7]. Modified stripes were found that suggested planar structures. The stripes were perpendicular to the laser field direction. Their spacing was found to depend on the pulse energy, and the number of laser pulses.

We confirm that the stripes are projections of planes. They extend over the full depth of the modified zone and can be organized over long distances when the sample is scanned under a fixed laser focus. We show that the laser electric field direction controls their alignment for any scan direction. We find that self-organized nanostructures are formed over a specific pulse energy range. Below this range the modification is uniform [6] and above it the modification is disordered. The nanoplanes are spaced by $\lambda_0/2n$, where $n$ is the refractive index of fused silica and $\lambda_0$ is the free space wavelength, for both 800 and 400 nm light independent of pulse energy. The planes are $\leq 10$ nm in width.

Our experiment used 50 fs, 800 nm pulses containing a peak energy of up to 3 $\mu$J and produced at a repetition rate of 100 kHz. The beam could be frequency doubled to produce 400 nm light. The beam was focused with a 0.45 or 0.65 NA microscope objective 100 $\mu$m below the surface of the sample. We produced extended modified regions by translating the sample at 30 $\mu$m/s perpendicular to the direction of propagation of the laser beam. Any exposed region experienced a few thousand shots.

We varied the average laser power from 5 –150 mW by attenuating the laser beam with a variable density filter. We used a $\lambda/4$ waveplate followed by a polarizer to change the laser polarization with respect to the scan direction. The advantage with this arrangement is that the electric field remains constant and the pulse duration is not affected as the polarization is rotated. The beam was precompensated for dispersion in the optical elements.

The AFM scans in Fig. 1 show two different projections of a periodic nanostructure array. Figure 1(a) is obtained by cutting the dielectric block in the $XZ$ plane as defined in the inset. The electric field ($\mathbf{E}$) of the laser pulse is polarized

 

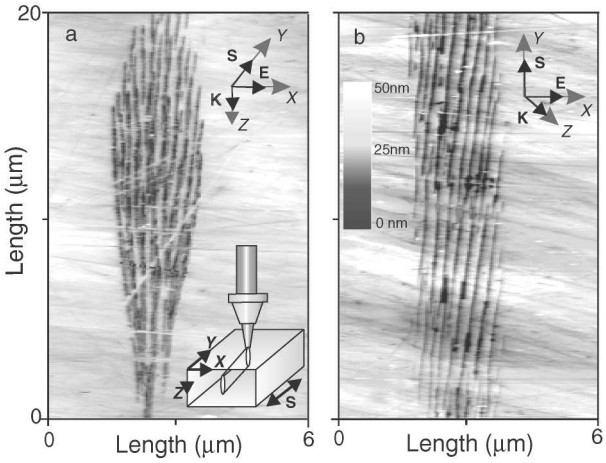


FIG. 1. Atomic force microscope images of chemically etched (4 min in 1% HF) laser-modified regions. The laser polarization is perpendicular to the scan direction. **K** is the direction of propagation of the laser radiation, **E** is the direction of electric field of the laser, and **S** is the scan direction. (a) Cross sectional view (in the $XZ$ plane) of the laser-modified region. (b) Top view (in the $XY$ plane) along the length of the modified region. The pulse energy is 250 nJ. The inset in (a) gives the experimental configuration and defines the coordinate axes.

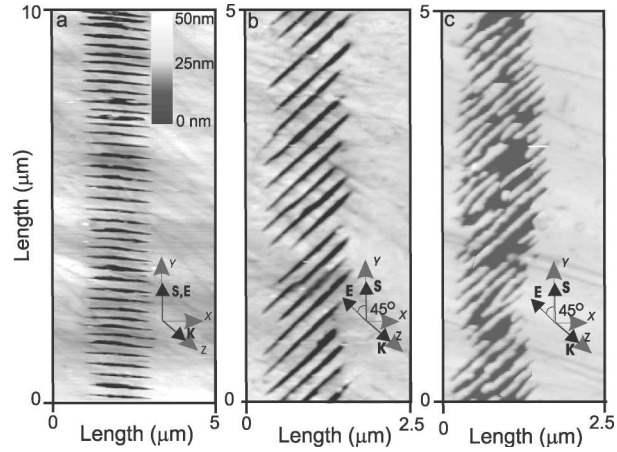


FIG. 2. AFM images (viewed from top of the sample) of chemically etched (4 min in 1% HF) modified regions with laser polarization at 0° (a) and 45° (b), and (c) with respect to the scan direction. Images (a) and (b) were obtained with 800 nm irradiation and with 400 nm in (c). The pulse energy was 300 nJ at 800 nm and 150 nJ at 400 nm.

close to the $X$ direction, approximately perpendicular to the scan direction. This end view shows that the planes extend over $\sim 20$ $\mu$m in the direction of laser light propagation. We expect the modification to occur preferentially in the region before the laser focus due to depletion of the pulse energy by nonlinear absorption [8].

Figure 1(b) is obtained by grinding and polishing the dielectric block in the $XY$ plane. This top view shows that the planes extend several tens of microns, limited by the slight angle between **E** and the $X$ axis.

We now demonstrate directly that changing the polarization of the laser with respect to the writing direction controls the orientation of the nanoplanes. Figure 2(a) shows an AFM image (viewed from the top of the sample) of modified planes obtained for linearly polarized light with **E** pointed along the scan direction. A long-range grating pattern is formed over the entire 1/2 cm writing range. This is remarkable because the sample moves essentially continuously, yet the grating pattern has not washed out. Instead, the coherence of the grating is continuously transferred as the sample is scanned. The average grating spacing is $242 \pm 10$ nm while $\lambda_0/2n = 276$ nm ($\lambda_0 = 800$ nm; $n = 1.45$, the refractive index of fused silica). The spacing is independent of pulse energy as shown in Fig. 3 [9].

Figure 2(b) is an AFM image (viewed from the top of the sample) of modified planes obtained for linearly polarized light with **E** directed at $\sim 45°$ to the scan direction. Long-range order is again evident, but the grating planes are tilted with their normal aligned to the polarization direction. This emphasizes the degree of control that the laser polarization gives over the grating alignment. Gratings are not produced with circularly polarized light.

The images in Figs. 1 and 2 do not reveal the true width of the nanoplanes. AFM depth profiles show that the planes are $<20$ nm wide, the resolution limit of the measurement. SEM images of very gently etched structures show the width to be $<10$ nm [Fig. 4(a)]. SEM images of structures that have been etched more strongly [Figs. 4(b) and 4(c)] provide a further demonstration of the 3-dimensional structure of the arrayed nanoplanes.

The structures shown in Fig. 2(a) are self-organized Bragg gratings. The material between the planes shows almost no modification with an etch rate less than 10% of the rate inside the planes—often much less [Fig. 3(a)]. It has been shown [6] that the etch rate in fs-laser-modified fused silica is proportional to the refractive index change of the material. If this still holds for the nanoplanes, then the index modulation in the grating is more than an order of

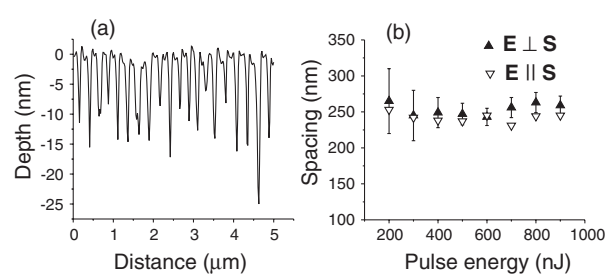


FIG. 3. Nanoplane spacing. (a) AFM line profile along the scan direction obtained from the scan shown in Fig. 2(a). (b) Nanoplane spacing as a function of pulse energy for **E** ⊥ **S** (▲) and **E** ∥ **S** (▽). The spacings and their variance was obtained from line profiles similar to that shown in (a). The variance for **E** ⊥ **S** is shown as the vertical bars. For **E** ∥ **S** it is ±10 nm.

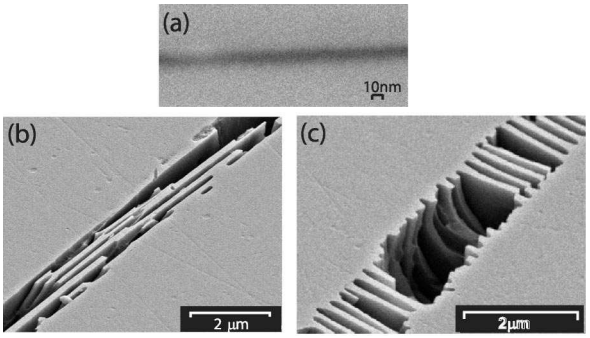


FIG. 4. Scanning electron microscope images of chemically etched laser-modified regions that have been overlayed with 1.5 nm Pt to avoid surface charging. (a) High resolution image of a weakly etched (20 s in 1% HF) structure written with **E** perpendicular to the scan direction, **S**; (b) and (c) are arrayed nanostructures written with $\mathbf{E} \perp \mathbf{S}$ and $\mathbf{E} \parallel \mathbf{S}$, respectively, after extensive etching (20 min in 1% HF) and disruption by ultrasonic cleaning.

magnitude larger than index changes generally made in UV-laser fabricated Bragg gratings. The relatively high etch rate may be indicative of severe local changes in the dielectric structure and may even imply dislocations.

The existence of ordered nanoplanes requires major modifications in the standard ideas of how dielectrics breakdown [4,5]. One proposal is that the planes result from interferences between the light and plasma waves [7]. The spacing is predicted to be dependent on the plasma temperature, $T_e$, and density, $N_e$. However, the $T_e(\sim 10^7$ K) and $N_E$ (asymtotically close to the critical density, $N_{\rm cr} = 1.75 \times 10^{21}$ cm$^{-3}$) conditions implied by this model are not consistent with the energy budget that arises from our 3D characterization of the modified region. There is just insufficient energy in the laser pulse to reach even close to the implied $T_e$. Estimating the volume of the modification as 30 $\mu$m$^3$ from Fig. 1, a pulse energy of 11 $\mu$J is required to reach $T_e \sim 10^7$ K at $N_e \sim 1.7 \times 10^{21}$ cm$^{-3}$. The structures are formed with energies as low as 200 nJ. The low threshold is consistent with our expectation that electron-ion collisions restrict $T_e$ to the order of the band gap ($\sim$10 eV).

We propose that the planes arise from local field enhancements that occur during inhomogeneous breakdown. This is based on ideas arising from nanoplasmonics. The very existence of nanoplanes that develop over thousands of laser shots requires that there is a memory in the material that can feed back to the breakdown. Such a memory could arise from metastable color centers [10] or permanent changes in electronic structure associated with chemical reorganization [11]. Either of these processes could seed localized ionization around areas that have already been modified. Without the memory, the ionization would be homogeneous.

Compared to the metal structures normally considered in nanoplasmonics, breakdown nanoplasmas start as underdense plasmas, they have no fixed boundaries and have a density gradient at the boundary. The internal electric field inside an underdense plasma exceeds the laser field. This enhances the local nature of the breakdown. There is positive feedback since the rate of plasma formation increases as the density increases. Shot to shot memory allows the feedback to work over many pulses. Thus nanoplasmas may grow even from thermal noise.

It is possible that the breakdown is inhomogeneous even on the first shot for two reasons. Natural inhomogeneties in the dielectric such as color centers and defects might form nucleation centers for nanoplasmas. In addition, the "forest-fire" multiphoton and avalanche ionization model, recently calculated for argon clusters, could form highly inhomogeneous plasmas [12].

Nanoplasmas naturally grow into nanoplanes when formed by linearly polarized electric fields. Consider an underdense spherical nanoplasma (Fig. 5). The boundary conditions require that the electric field around the equator (as defined in the figure) is enhanced and the electric field at the poles is suppressed [13,14]. When the plasma density is half the critical value [3] the relative field enhancement is a factor of 2 and increases significantly as the critical density is approached. Even small changes in the field have a large effect on highly nonlinear multiphoton ionization. Thus, underdense nanoplasmas must grow into nanosheets orientated with their normal parallel to the laser polarization, just as we observe. Since the plasma is unconstrained, growth will continue at the edges without limit. It may appear that this peripheral growth would halt when the plasma density exceeds the plasma resonance (the critical density for a bulk plasma or for a large plasma sheet).

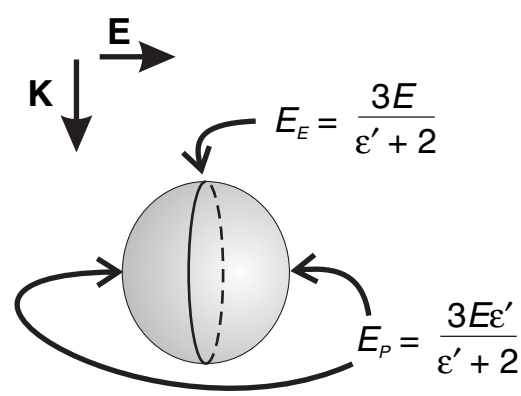


FIG. 5. Schematic showing local field enhancement outside a nanoplasma. **K** denotes the direction of propagation of the laser beam and **E** the electric field. $E_E$ and $E_P$ are the local fields found at the equator and poles of the sphere, respectively, for an overall field $E$. $\varepsilon'$ is the ratio of the permitivities of the nanosphere and the dielectric medium. When $\varepsilon' < 1$ (i.e., when the plasma density is less than the critical density), field enhancement occurs around the equator and the spherical nanoplasma expands to form an oblate ellipsoid that evolves into a nanoplane.

However, this is not true. In unconstrained plasmas, the plasma boundaries are graded and the critical density is never exceeded at any boundary.

We have extended our nonlinear absorption measurements made on borosilicate glass [8] to fused silica. We find that, at the threshold for nanoplane formation (200 nJ), 50% of the beam is absorbed. From this we estimate that the average carrier density is $10^{21}$ cm$^{-3}$, assuming that the light is absorbed in the volume of the modified region in Fig. 1, that the electron temperature is the band gap energy ($\sim$9 eV) and that recombination plays no role on these short time scales. If the planes are $\sim$10 nm thick and absorption is confined to the planes, this implies that the plasma density within the sheets reaches $2.5 \times 10^{22}$ cm$^{-3}$. At such densities recombination could be very fast—the rates are not known. However, it seems safe to assume that the critical density is exceeded. In this case the sheets must affect light propagation; for a single sheet, surface plasmons will be excited and for multiple sheets, the light must adopt modes similar to those established in planar metallic waveguides.

The order naturally evolves from a random distribution of nanoplasmas over many shots due to the memory mechanism and mode selection. Planes will be favored only if they support modes whose field distribution reinforces their own growth. Although a great deal of work is required to understand this in detail, the $\lambda_0/2n$ plane spacing is reminiscent of the minimum spacing required in a planar metal waveguide to support such modes having field maxima at the metal-dielectric interface. It is likely that transient plasma based planar waveguides have similar properties favoring their development from an initially random nanoplasma distribution.

In conclusion, the nanoplasmonic model that we propose explains many observations. First, the formation of nanoplanes and their orientation is easily understood in terms of local field enhancements. Second, the scaling of the array spacing with $\lambda$ follows naturally if the order is imposed by modes related to planar waveguides. Third, since the spacing is imposed by the mode structure, a dependence on pulse energy is not expected. Finally, as the laser focus moves, order is imposed in the newly exposed material by the modes of the plasma grating seeded by the existing nanostructure.

Our results highlight the need for fundamental measurements on high-density plasmas in transparent media. For example, even such fundamental properties as Auger and other recombination rates are not measured at densities approaching those that are important for dielectric modification. Electrons interacting with solids in the presence of strong laser fields are poorly understood. Modes in nonmetallic lossy, transient waveguides have not been considered.

We thank M. Stockman and M. Yu. Ivanov for valuable discussions. This work was supported in part by NRC-British Council Collaboration.

*Present address: Department of Physics, University of Ottawa, 150 Louis Pasteur, Ottawa, K1N 6N5, Canada.
†Electronic address: david.rayner@nrc-cnrc.gc.ca
‡Electronic address: paul.corkum@nrc-cnrc.gc.ca

[1] W. L. Barnes, A. Dereux, and, T. W. Ebbesen, Nature (London) **424**, 824 (2003); P. Andrew and W. Barnes, Science **306**, 1002 (2004).
[2] K. Li, M. I. Stockman, and D. J. Bergman, Phys. Rev. Lett. **91**, 227402 (2003).
[3] In an underdense plasma, the electron density is less than the critical density ($1.75 \times 10^{21}$ cm$^{-3}$ at our laser frequency) above which the plasma becomes reflective.
[4] X. Liu, D. Du, and G. Mourou, IEEE J. Quantum Electron. **33**, 1706 (1997); D. Du, X. Liu, G. Korn, J. Squier, and G. Mourou, Appl. Phys. Lett. **64**, 3071 (1994); B. C. Stuart *et al.*, Phys. Rev. B **53**, 1749 (1996).
[5] M. Lenzner *et al.*, Phys. Rev. Lett. **80**, 4076 (1998); M. Li, S. Menon, J. P. Nibarger, and G. N. Gibson, Phys. Rev. Lett. **82**, 2394 (1999).
[6] R. S. Taylor *et al.*, Opt. Express **11**, 775 (2003).
[7] Y. Shimotsuma, P. G. Kazansky, J. Qiu, and K. Hirao, Phys. Rev. Lett. **91**, 247405 (2003).
[8] D. M. Rayner, A. Naumov, and P. B. Corkum, Opt. Express **13**, 3208 (2005).
[9] This observation is based on our 3D measurements and pertains through the bulk of the structures. It contradicts the finding of Shimotsuma *et al.* that the spacing is pulse energy dependent (Ref. [7]). It is possible that their 2D images were obtained mainly in the top of the laser-modified regions where we observe nonsystematic variation of the spacing with pulse energy.
[10] L. Skuja, H. Hosono, and M. Hirano, Proc. SPIE-Int. Soc. Opt. Eng. **4347**, 155 (2001).
[11] J. W. Chan, T. Huser, S. Risbud, and D. M. Krol, Opt. Lett. **26**, 1726 (2001).
[12] L. N. Gaier *et al.*, J. Phys. B **37**, L57 (2004).
[13] J. D. Jackson, *Classical Electrodynamics* (Wiley, New York, 1975), 2nd ed.
[14] G. T. Boyd, T. Rasing, J. R. R. Leite, and Y. R. Shen, Phys. Rev. B **30**, 519 (1984).